JOURNAL OF SOLID STATE CHEMISTRY 112, 106–112 (1994)

Crystal Structure of Silicon Pyrophosphate (Form I) from Powder Diffraction Data

D. M. Poojary, R. B. Borade, F. L. Campbell III, and A. Clearfield[1]

Department of Chemistry, Texas A&M University, College Station, Texas 77843

Received July 29, 1993; in revised form November 22, 1993; accepted November 23, 1993

The crystal structure of silicon pyrophosphate (Form I) was solved from X-ray powder data and refined by the Rietveld method. The crystals belong to the hexagonal space group $P6_3$ with a = 4.7158(3) Å and c = 11.917(1) Å. There are two SiP_2O_7 units in the unit cell. Both the P atoms and the Si atom are located on threefold axes. The silicon atoms are situated in the ab plane at $z = 0$ and $\frac{1}{2}$. One of the P atoms of the pyrophosphate group is located slightly above the plane at $z = 0$ while the other is slightly below the plane at $z = \frac{1}{2}$. Thus, the structure resembles the layer structure of α-zirconium phosphate. The layers in the present case, however, are held together by the P–O–P bonds. The relationship between this structure and those of the other pyrophosphates and the layered $M(HPO_4)_2$ phases is discussed.

INTRODUCTION

A large number of silicon pyrophsophates have been reported in the literature, all of composition SiP_2O_7. It is of interest to explore how a compound of such seemingly simple composition can have so many polymorphs. We have listed in Table 1 the different phases of this composition that appear in the literature. The crystal structures of phases AIII and AIV and the cubic phases have been determined (5–7). These phases were all prepared at high temperatures. For example, phase AIII was obtained by heating a precipitated silicon phosphate gel in a sealed quartz tube with a temperature gradient of 800 to 1000°C. Needle-shaped crystals collected in the cool end of the tube (5). Phase AIV was prepared by dissolving finely divided silica in concentrated phosphoric acid at 250°C and precipitating a solid by long heating at 200°C. This solid was then heated in a sealed quartz tube at 950°C for 64 hr (6). The cubic SiP_2O_7 crystals were grown by a transport reaction from $Li_{0.25}Al_{0.25}Si_{0.75}P_2O_7$ in a platinum tube (7). The hot end of the tube was kept at 1000°C for 3 days whereas the colder end of the tube had a temperature of 960°C.

[1] To whom correspondence should be addressed.

The remaining pyrophosphates were prepared at lower temperatures in the range of 300–600°C (2). It was of interest to see how the structures of the low-temperature preparations differ from those of the high-temperature phases. We were able to prepare the compound designated as Form I in Table 1 and to solve its structure from X-ray powder data. The results are described here and the relationship of this phase to other silicon and zirconium phosphates is developed under Discussion.

SYNTHESIS

For the preparation of SiP_2O_7, 40 g of 85% phosphoric acid (Fisher reagent grade) was heated at 250°C for 5 hr, during which time it lost 19.6% of its weight. To this concentrated P_2O_5 solution (76.6% P_2O_5) was added 5.46 g of finely divided SiO_2 (95%, M1L-D, Davison Chemical Co.) and the mixture kept at 120°C for 40 hr. Then the temperature was held at 250°C for 24 hr. This mixture was then cooled to room temperature and ethanol added. It was then filtered and the solid washed extensively with ethanol and then dried at 40°C. Its X-ray diffraction pattern was identified as that of the hexagonal Form I of Makart (2). Also present was about 10% of a second phase tentatively identified as Makart's Form III.

DATA COLLECTION, STRUCTURE SOLUTION, AND REFINEMENT

Step-scanned X-ray powder data were collected at room temperature on a finely ground sample of silicon pyrophosphate by using a Rigaku computer-automated diffractometer. The X-ray source was a rotating anode operating at 50 kV and 180 mA with a copper target and graphite monochromated radiation (λ = 1.54185 Å). Data were collected between 10° and 120° in 2Θ using a 0.5° divergence slit with a step size of 0.02° and a count time of 10 sec per step. The data were transferred to a DEC Micro-VAX-II computer and the pattern was decomposed as described earlier (8). Indexing was carried out using

0022-4596/94 $6.00

TABLE 1
Known or Reported Phases of SiP_2O_7

Phase designation	Crystal system	Unit cell dimensions				Ref.
		a (Å)	b (Å)	c (Å)	β (°)	
AIII	Monoclinic	4.73	6.33	14.71	90.1	1
AIV (form II)	Monoclinic	4.733(5)	12.019(9)	7.654(7)	91.03(9)	1, 2
Form III	Tetragonal	14.20	—	7.39	—	2
AII	Tetragonal	22.36	—	14.91	—	1
Form I	Hexagonal	4.72	—	11.82	—	2
BI	Hexagonal	8.18	—	11.85	—	1
Form IV	Cubic	7.473(1)	—	—	—	1–3
AI	Cubic	22.418(2)	—	—	—	1, 4

trial and error methods (9) and refined by least-squares methods. The indexed pattern showed reflections of the type $00l$ with l odd absent indicating that the space group is $P6_3$ or $P6_3/m$. There were 40 singly indexed reflections up to a 2Θ limit of 70°. This data set was used to generate the normal $F_0(hkl)$ and $\sigma(F_0)$ for structure solution. A Patterson map was computed in the space group $P6_3$ using the program SHELXTL PLUS (10). The positions of the silicon and phosphorus atoms were derived from this vector map. These positions were the heaviest peaks in the E map obtained using the same data set as that in the program TEXSAN (11). The positions of the oxygen atoms were located from the subsequent difference Fourier maps. The P, Si, and oxygen atom linking the P atoms are all located on the threefold axes.

These positional parameters were used as a starting model for the Rietveld refinement. Using a utility program, GRAPH (12), the raw data were transferred to the GSAS (13) program package for the Rietveld method of full-profile refinement. The pairs of peaks arising from the $\alpha 1$ and $\alpha 2$ doublet were treated as separate reflections in the fixed intensity ratio of 2 : 1. In both cases, the refinement was started with the profile coefficients obtained from the refinement of lanthanum boride powder data which were collected on the same instrument. Initial refinement of the scale, background (three parameters), unit cell parameters, and the zero point error led to good agreement between the observed and calculated patterns, indicating that the starting structural model is correct. Careful refinement of the profile function (pseudo-Voigt; number of coefficients = 11) and increasing the background coefficients to 12 showed a considerable improvement in the calculated pattern. Atomic positions were then refined with soft constraints consisting of both Si–O and P–O bond distances and O–O nonbonded distances. P–O distances were constrained to be 1.53 Å and Si–O distances to be 1.73 Å. The allowable refinement bound in both cases was 0.2 Å. The geometry around Si and P was obtained by the appropriate distances between the bonded oxygen atoms. A total of 12 geometric constraints was included and initially their weight was kept high to maintain a reasonable geometry. Although it is a common practice to input a set of geometric constraints for a stable refinement, in this case it was necessary because the structure appears to be pseudo-symmetric. As the refinement progressed the soft constraints were assigned less and less weight but they could not be removed completely. The final agreement factors were $R_{wp} = 0.20$, $R_p = 0.15$, and $R_F = 0.16$. These large errors result from the presence of about 10% of an impurity phase (Form III) (see Table 1). Peaks which could be identified as solely due to the impurity were removed from the pattern for the refinement. However, no corrections were made for the intensities of those peaks which overlap with the reflections from the impurity phase.

In the refined structure, it appears that the P and oxygen atoms (O1 and O3) are related by the operation x, y, $\frac{1}{2}$-z, although the deviation is much larger in the case of oxygen positions. Therefore, attempts were made to refine the structure in the centric space group, $P6_3/m$. In this space group, the Si atom lies on a $\bar{3}$-axis, O_2 on a $\bar{6}$-axis, and the P atom on a threefold axis. An oxygen atom, either O1 or O3, in the general position completes the asymmetric part of the structure. Although most of the calculated intensities matched closely with those in the observed pattern, the refinement stopped at $R_{wp} = 0.26$ and therefore was deemed not as good as that in the space group $P6_3$. The refinements however suggest the possibility of the structure being pseudo-symmetric. The presence of the impurity phase further complicates this problem. In the case of $P6_3/m$ the oxygen atom O2 must be constrained at $\frac{2}{3}$, $\frac{1}{3}$, and $\frac{1}{4}$, and the x- and y-coordinates of O1 and O3 should be made equal. These constraints in turn distort the geometry of the pyrophosphate group during the refinement. It may also be possible that O2 is disordered in order to attain a nonlinear P–O–P bond which is commonly observed in most of the pyrophosphate structures. This feature is not apparent in the difference Fourier map

which does not support either of the possibilities given the quality and the resolution of the diffraction data.

In order to determine whether SiP_2O_7 (Form I) would convert to other pyrophosphate structures at elevated temperatures a high-temperature X-ray study covering the range of 300 to 1100°C was carried out. A Rigaku high-temperature camera was used in conjunction with a Rigaku *RU200* rotating anode X-ray diffractometer. The radiation was Cu$K\alpha$ (λ = 1.5418 Å). The sample was heated to 300°C at the rate of 1°/min and held there for 10 min, and the pattern was recorded. A second scan was recorded 1 hr after the first to determine whether a slow transformation occurred. This process was repeated every 100 to 1100°C.

RESULTS

Crystallographic data are listed in Table 2 while the final positional and isotropic thermal parameters are given in Table 3. A list of the bond lengths and angles is presented in Table 4. The coordination about the silicon atom, the geometry of the P_2O_7 group, and the numbering scheme used in the tables are shown in Fig. 1. Incomplete arrangement of the atoms in one unit cell is shown in Fig. 2. Some of the atoms, such as the remaining Si atom at the corners of the unit cell, were omitted in this figure for clarity.

The Si atoms lie on a threefold axis and they are octahedrally coordinated by symmetry-related O(1) and O(3) atoms. The oxygen atoms which bond to any one silicon atom originate from six different pyrophosphate groups. This in turn requires that each pyrophosphate group bond to six different silicon atoms. The Si atoms are located in the *ab* planes at $z = 0$ and $\frac{1}{2}$ (Figs. 2 and 4). Three silicon atoms which form an equilateral triangle are joined through bridging by a $-PO_3$ group (Fig. 2). These bridging groups are alternately above and below the *ab* plane (Fig. 4) and rotated by the threefold axis to create the octahedral coordination about the silicon atoms. This bridging sequence is very similar to that observed in the well-known α-zirconium phosphate (14, 15). The three oxygen atoms of each end of the pyrophosphate bond to similar Si equilateral triangles in adjacent layers such that the two groups are almost in an eclipsed conformation (Fig. 3) while the P–O–P bonds form linear bridges between the layers (Fig. 4). The PO_4 groups show regular geometry with average bond lengths and angles. The P–O distances range from 1.48 to 1.58 Å (average value = 1.52 Å) and the tetrahedral angles are in the range 103°–115°. The Si atoms display regular octahedral geometry with an average Si–O bond length of 1.735 Å. The *cis* angles in SiO_6 octahedra range between 80° and 102° while the *trans* angle is 165°. The eclipsed nature of the pyrophosphate group is shown by the torsion angles, O1–P2–O2–P1–O3, of 14.7°. A Rietveld refinement of this geometry is shown in Fig. 5.

TABLE 2
Crystallographic Data

Pattern range (2θ) (°)	13.7–92
Step scan increment (2θ) (°)	0.02
Step scan time (sec)	10
Space group	$P6_3$
a (Å)	4.7158(3)
b (Å)	4.7158(3)
c (Å)	11.917(1)
Z	2
D_{calc}, (mg m^{-3})	2.226
No. of contributing reflections	146
No. geometric observations	12
P–O distances and tolerance (Å)	1.53(2)
Si–O distances and tolerance (Å)	1.73(2)
O–O distances for PO_4 (Å)	2.55(2)
No. of structural parameters	9
No. of profile parameters	11
Expected R_{wp}, χ^2	0.02, $\sqrt{10}$
R_{wp}	0.20
R_p	0.15
R_F	0.16

Note. $R_{wp} = (\Sigma\, w(I_o - I_c)^2/\Sigma\, [wI_o^2])^{1/2}$, $R_p = (\Sigma\, |I_o - I_c|/\Sigma\, I_c)$, expected $R_{wp} = R_{wp}/(\chi^2)^{1/2}$, $\chi^2 = \Sigma\, w(I_o - I_c)^2/(N_{obs} - N_{var})$, $R_F = \langle |F_o| - |F_c| \rangle / \langle |F_o| \rangle$.

TABLE 3
Positional and Thermal Parameters

Atom	x	y	z	U_{iso} (Å^2)
Si	0	0	0	0.002(3)
P1	$\frac{2}{3}$	$\frac{1}{3}$	0.394(2)	0.009(5)
P2	$\frac{2}{3}$	$\frac{1}{3}$	0.133(2)	0.009(4)
O1	0.859(4)	0.178(3)	0.100(2)	0.025(6)
O2	$\frac{2}{3}$	$\frac{1}{3}$	0.261(2)	0.046(7)
O3	0.930(2)	0.261(4)	0.422(2)	0.036(6)

Note. $U_{iso} = B_{iso}/8\Pi^2$.

TABLE 4
Bond Lengths (Å) and Angles (°)

Si–O1	1.77(1)	3×	O1–Si–O1	81(1)	3×
Si–O3	1.70(2)	3×	O1–Si–O3	86(1)	3×
			O1–Si–O3	102(1)	3×
			O1–Si–O3	165(1)	3×
			O3–Si–O3	93(1)	3×
P1–O2	1.58(2)		O2–P1–O3	103(1)	3×
P1–O3	1.48(1)	3×	O3–P1–O3	115(1)	3×
P2–O2	1.53(2)		O1–P2–O2	105(1)	3×
P2–O1	1.48(1)	3×	O1–P2–O1	113(1)	3×
P1–O1–Si	152(2)		P2–O2–P1	180	
P1–O3–Si	141(1)				

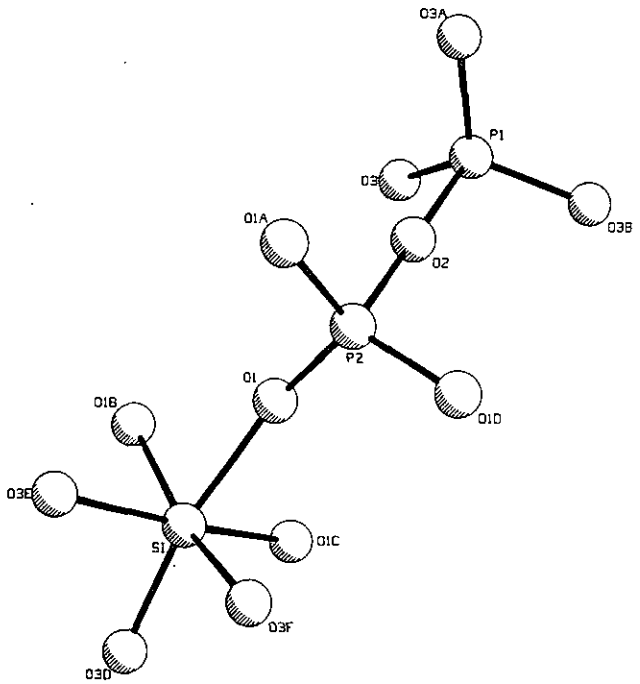

FIG. 1. Ball and stick schematic of a single SiP_2O_7 unit used in the tables.

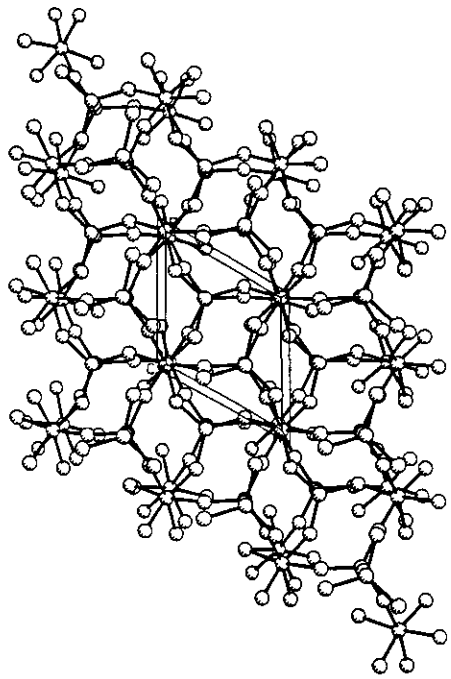

FIG. 3. Packing of the molecules as viewed down the *c* axis.

Because SiP_2O_7 can exist in one of several high-temperature phases, it was of interest to determine whether Form I would undergo a phase transformation at elevated temperatures to one of the known high-temperature structures. As was already indicated, a small percentage of Makart's preparation (Form III, Table 1) was present together with the main phase. It was suspected that Form I might transform to Form III followed by a further phase transformation to one of the high-temperature phases. The results of the high-temperature study are shown in Fig. 6. It is seen that there is no change in the X-ray pattern until 1000°C. In fact, the peaks for the minor phase, Form III, are also presently unchanged. This

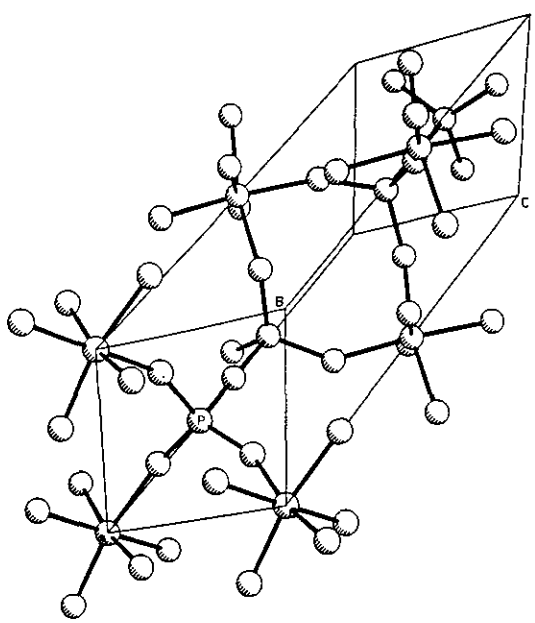

FIG. 2. Packing of the molecule in the unit cell showing the bridging of Si atoms by phosphate groups.

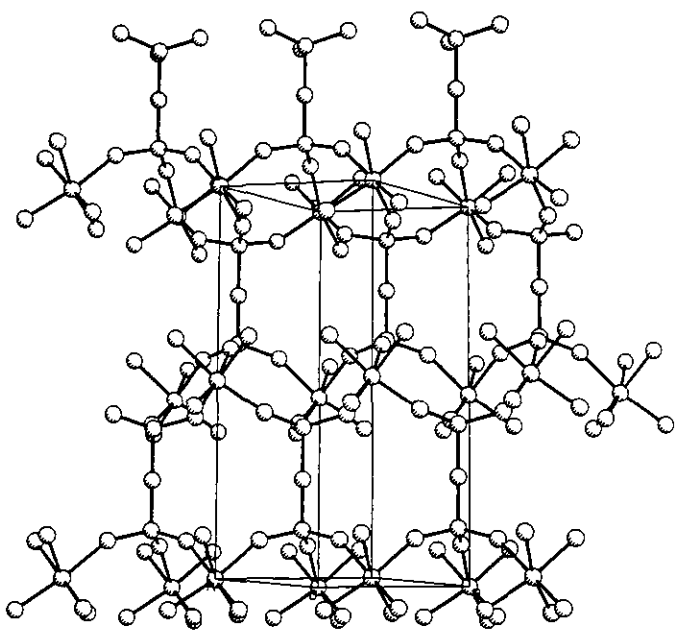

FIG. 4. Packing of the molecules as viewed down the *a* axis showing the arrangement of layers bridged by P–O–P bonds.

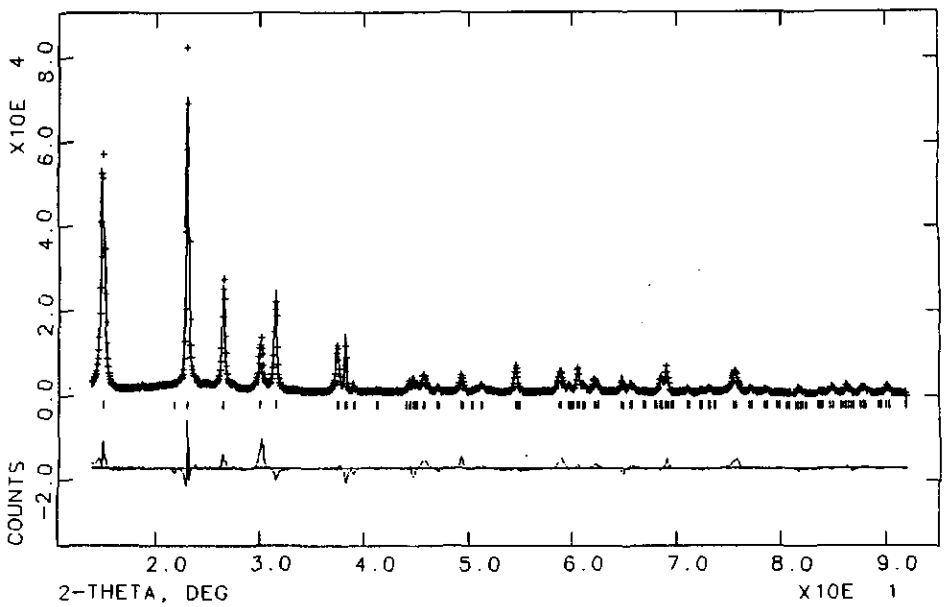

FIG. 5. Observed (+) and calculated (−) profiles (X-ray intensity versus 2θ) for the Rietveld refinement. The bottom curve is the difference plot on the same scale.

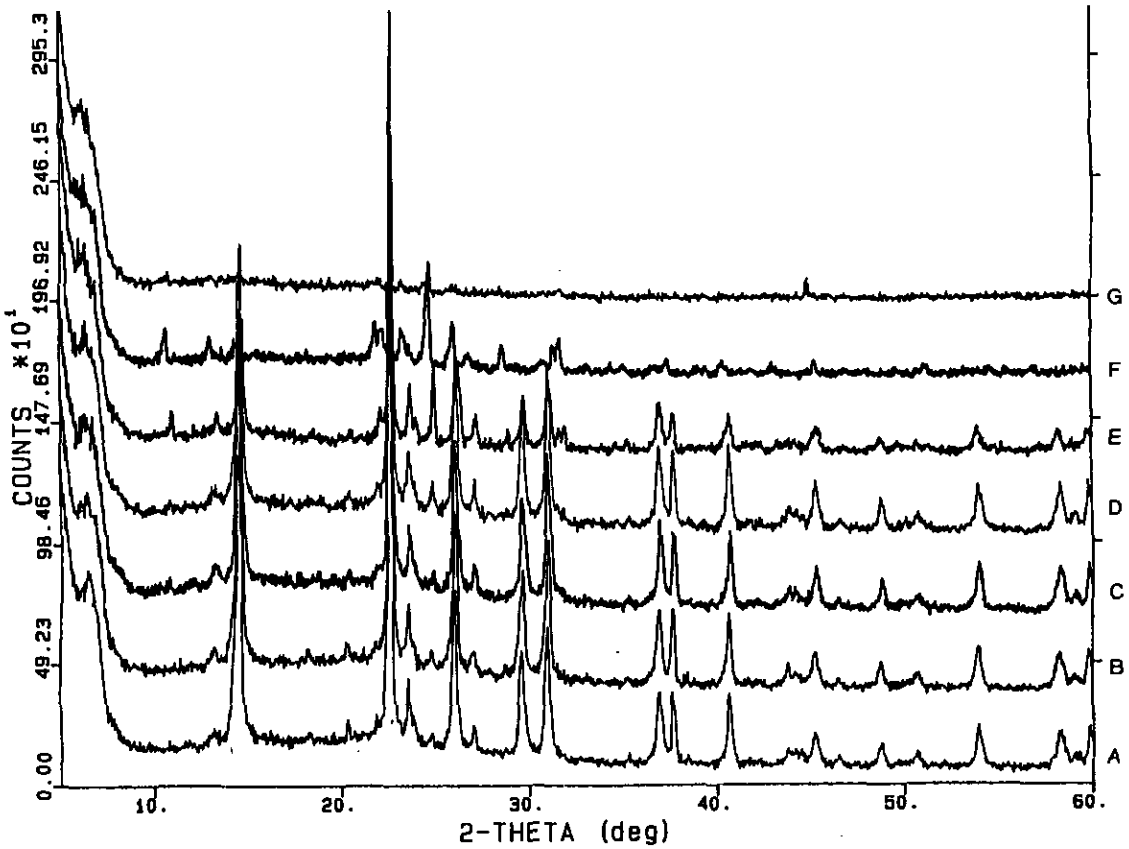

FIG. 6. X-ray powder patterns of SiP_2O_7 at elevated temperatures: (A) 500°C, (B) 600°C, (C) 700°C, (D) 800°C, (E) 900°C, (F) 1000°C, (G) 1100°C.

means that each of these pyrophosphate phases is stable to 900°C without converting into each other. However, a new X-ray pattern begins to form at 1000°C. The *d* spacings correspond to those of the silicon phosphate of composition $Si_5O(PO_4)_6$ (22). This transformation requires a considerable loss of P_2O_5 from the pyrophosphate and cleavage of the pyrophosphate groups to form PO_4^{3-} ions. Such a high-energy reaction is remarkable since it occurs in preference to what might be considered a low-energy transformation to another SiP_2O_7 phase.

DISCUSSION

This study has revealed certain analogies between the zirconium phosphate, pyrophosphate system and that of silicon. The well-known α-zirconium phosphate, $Zr(HPO_4)_2 \cdot H_2O$, is layered (14) and has a layered silicon analogue (16–18). The zirconium compound dehydrates at about 100°C and then above about 400°C condenses with loss of another mole of water to form a poorly crystalline phase (19, 20). Alberti and Constantino (21) interpreted the weak reflections of this solid on the basis of a condensation between P–OH groups in adjacent layers to form a pyrophosphaste as shown in Fig. 7. This structure is very similar to that of the silicon pyrophosphate (Form I) determined by this study. The metal atoms are six coordinated, being bonded to six different phosphate groups. Each phosphate group bridges across three metal atoms and the fourth oxygen forms the P–O–P bond, which makes a 180° angle. Thus, it would appear that silicon pyrophosphate, Form I, is the first condensation product of the layered silicon phosphate, $Si(HPO_4)_2 \cdot H_2O$. Although the layered compounds are monoclinic ($P2_1/c$ or $P2_1/n$) they can also be described on the basis of a pseudo-hexagonal lattice (14). Only a very slight shifting of atoms is necessary to convert the monolayered hydrogen phosphates into the hexagonal pyrophosphate (Form I).

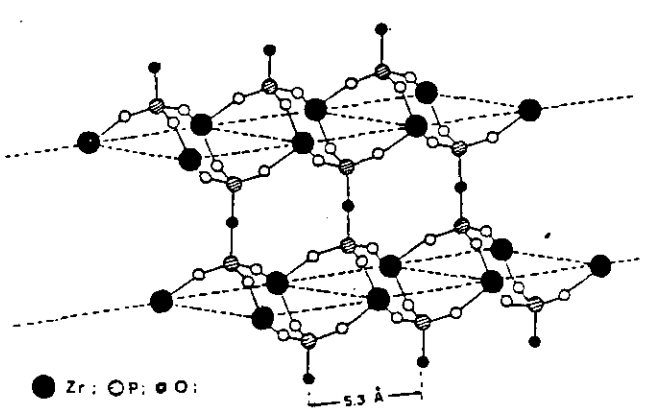

FIG. 7. Schematic representation of the poorly crystalline ZrP_2O_7 as depicted in Ref. (21).

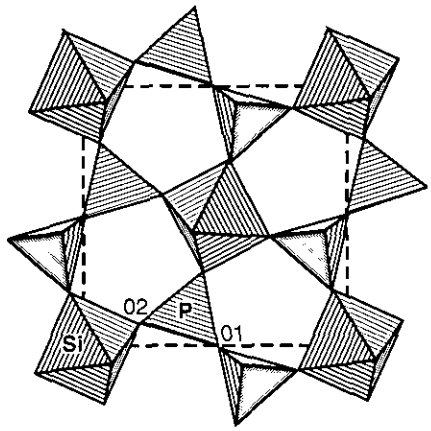

FIG. 8. Polyhedral representation of the cubic subcell of SiP_2O_7 (from Ref. 7).

To determine whether the zirconium phosphate formed a pyrophosphate of the type pictured in Fig. 8, a sample of the layered α-phase was kept at 500°C for 96 hr. While An X-ray powder pattern developed, it was that of poorly crystalline material superimposed on a very high background. The pattern appears to be that of a mixture, one phase being the cubic pyrophosphate and the other the hexagonal pyrophosphate. Heating to 600 and 700°C did not change the pattern except to sharpen the reflections somewhat.

Further heating of this poorly crystalline zirconium pyrophosphate to above 700°C converts it (19, 20) into the cubic pyrophosphate described by Levi and Peyronel (3). This well-crystallized zirconium pyrophosphate also exhibits a superlattice of the type described by Tillmanns *et al.* (7) for cubic SiP_2O_7. In the superstructure, the subcell of 7.47 Å is tripled and thus has a volume 27 times that of the substructure. There are 4 SiP_2O_7 units in the small cell and 108 in the supercell (7). The small cell has a sodium chloride-type structure with silicon octahedra at the corners and face centers of the cube and the central oxygen of each pyrophosphate group lying halfway along the cell edges as shown in Fig. 8. In this unit cell SiO_6 octahedra lie along the face diagonal with the pyrophosphate coordination similar to that in the Form I compound. The arrangement is the same along both face diagonals, making the face a square. A major difference is that the pyrophosphate is in a staggered conformation rather than eclipsed although the P–O–P angle is still 180°. The subcell length is then approximately $A_{\text{cubic}} \cong C_{\text{hexagonal}}/\sqrt{2}$. Thus, a considerable rearrangement of the phosphate groups must take place to form the cubic phase and much higher temperatures are required. In the subcell all the P–O–P angles are constrained to be 180° by symmetry. However, in the larger supercell the average value of this angle is 150°. Bending of the pyrophosphate groups in different directions is responsible for the supercell. The

appearance of straight P–O–P bonds is the result of positional disorder of the bent pyrophosphate groups (7). In the bent conformation an eclipsed configuration is energetically highly unfavorable so the staggered conformation is adopted. In the hexagonal (Form I) structure the silicons in one layer are separated by $c/2$ from those in an adjacent layer connected by a pyrophosphate bridge. This distance is 5.91 Å in Form I and 5.28 Å in the cubic pyrophosphate, the difference arising from the bent conformation in the cubic phase.

The two monoclinic phases AIII and AIV are high-temperature phases with P–O–P angles of 139.2° and 132.3°, respectively, and staggered pyrophosphate conformations. They are prepared under very special conditions requiring the use of high temperatures for long periods of time (1, 2). As a result, neither the low-temperature hexagonal phase nor the tetragonal phase convert to the monoclinic phases. However, the ease of formation of the cubic phase for the group 4 and 14 metals would suggest that a hexagonal to cubic transformation should be facile. Why this transformation does not occur in the SiP_2O_7 system is a mystery, but may be connected with the small size of the Si^{4+} ion.

ACKNOWLEDGMENTS

This study was supported by United Catalysts Inc., Louisville, KY, to which grateful acknowledgment is made. We also thank Richard Carroll for carrying out the zirconium study.

REFERENCES

1. F. Liebau, G. Bissert, and N. Koppen, *Z. Anorg. Allg. Chem.* **359,** 113 (1968).
2. H. Makart, *Helv. Chim. Acta* **50,** 399 (1967).
3. G. R. Levi and G. Peyronel, *Z. Kristallogr.* **92,** 190 (1935).
4. H. Vollenkle, A. Wittmann, and H. Nowotny, *Monatsh. Chem.* **94,** 956 (1963).
5. G. Bissert and F. Liebau, *Acta Crystallogr. Sect. B* **26,** 233 (1970).
6. F. Liebau and K.-F. Hesse, *Z. Kristallogr.* **133,** 213 (1971).
7. E. Tillmanns, W. Gebert, and W. H. Baur, *J. Solid State Chem.* **7,** 69 (1973).
8. P. R. Rudolf and A. Clearfield, *Inorg. Chem.* **28,** 1706 (1989).
9. P.-E. Werner, *Z. Kristallogr.* **120,** 375 (1965).
10. G. M. Sheldrick, SHELXTL PLUS, Users Manual, Siemans Analytical X-Ray Inst., Madison, WI, 1989.
11. "TEXSAN, Texray Structure Analysis Package," Molecular Structure Corp., The Woodlands, TX, 1987 (revised).
12. P. R. Rudolf and A. Clearfield, "GRAPH," Texas A&M University, 1991.
13. A. Larson and R. B. von Dreele, "GSAS, Generalized Structure Analysis System," LANSCE, Los Alamos National Laboratory, Regents of the University of California, 1985–1988.
14. A. Clearfield and G. D. Smith, *Inorg. Chem.* **8,** 421 (1969).
15. J. M. Troup and A. Clearfield, *Inorg. Chem.* **16,** 3311 (1977).
16. A. Boullé and R. Jary, *C.R. Hebd. Seances Acad. Sci.* **237,** 161 (1953); **237,** 328 (1953).
17. J. Goubeau, K. D. Christe, W. Tlsk, and W. Wilborn, *Z. Anorg. Allg. Chem.* **325,** 26 (1963).
18. A. Winkler and E. Thilo, *Z. Anorg. Allg. Chem.* **346,** 92 (1966).
19. A. Clearfield and J. A. Stynes, *Inorg. Nucl. Chem.* **26,** 117 (1964).
20. A. Clearfield and S. P. Pack, *J. Inorg. Nucl. Chem.* **37,** 1283 (1974).
21. G. Alberti and V. Costantino, *J. Mol. Catal.* **27,** 235 (1984).
22. D. M. Poojary, R. B. Borade, and A. Clearfield, *Inorg. Chim. Acta* **208,** 23 (1993).